Spot-on: Safe Fuel/Air Compression

Jeffrey Banks, Joseph Fehribach, Alistair Fitt, Robert Hart, Kevin Hughes,
John Ockendon, Colin Please, Don Schwendeman, Burt Tilley, Suzanne Weekes

December 9, 2003

1 Introduction

The emission of fuel vapors into the atmosphere from underground storage tanks at filling stations is a common occurrence in many parts the world. The conditions of the vapor in the tanks vary significantly over a 24 hour period such that evaporation and excess air ingestion during the refueling process can cause tank over pressurization and subsequent emissions. At other times during a 24 hour cycle, pressures can fall below atmospheric pressure. The state of California has recognized this emissions problem and has enacted regulations to address it.

Due to these low-emission environmental requirements in California, solutions must be implemented that do not entail release of these vapors into the atmosphere. One solution requires that the vapors fill a balloon during the appropriate times. However, the size of the balloon at typical inflation rates requires a significant amount of physical space (approximately 1000-2000 liters), which may not necessarily be available at filling stations in urban areas. Veeder-Root has a patent pending for a system to compress the vapors that are released to a 10:1 ratio, store this compressed vapor in a small storage tank, and then return the vapors to the original underground fuel tank when the conditions are thermodynamically appropriate (see Figure 1 for the schematic representation of this system).

The limitation of the compressor, however, is that the compression phase must take place below the ignition temperature of the vapor. For a 10:1 compression ratio, however, the adiabatic temperature rise of a vapor would be above the ignition temperature. Mathematical modeling is necessary here to estimate the performance of the compressor, and to suggest paths in design for improvement.

This report starts with a mathematical formulation of an ideal compressor, and uses the anticipated geometry of the compressor to state a simplified set of partial differential equations. The adiabatic case is then considered, assuming that the temporary storage tank is kept at a constant temperature. Next, the heat transfer from the compression chamber through the compressor walls is incorporated into the model. Finally, we consider the case near the valve wall, which is subject to the maximum temperature rise over the estimated 10,000 cycles that will be necessary for the process to occur. We find that for adiabatic conditions, there is a hot spot close to the wall where the vapor temperature can exceed the wall temperature. Lastly, we discuss the implications of our analysis, and its limitations.

2 Problem Formulation

Consider the gas mixture in the domain $x_p^*(t^*) < x^* < L$, where the piston is located at $x = x_p^*(t^*)$ (see Figure 2. The piston has a stroke length $l^* < L$, and this length needs to be determined based on the overall compressor capabilities. Surrounding this gas in a cylindrical container are the compressor walls, found in the domain $a < r^* < a + b, 0 < x^* < L$ (for now we assume that the end walls do not play a specific role). The equations of motion for the gas are given by conservation of mass, conservation of momentum, conservation of energy, and an equation of state

$$\rho_{t^*}^* + \nabla \cdot (\rho^* \mathbf{u}^*) = 0 \tag{1}$$

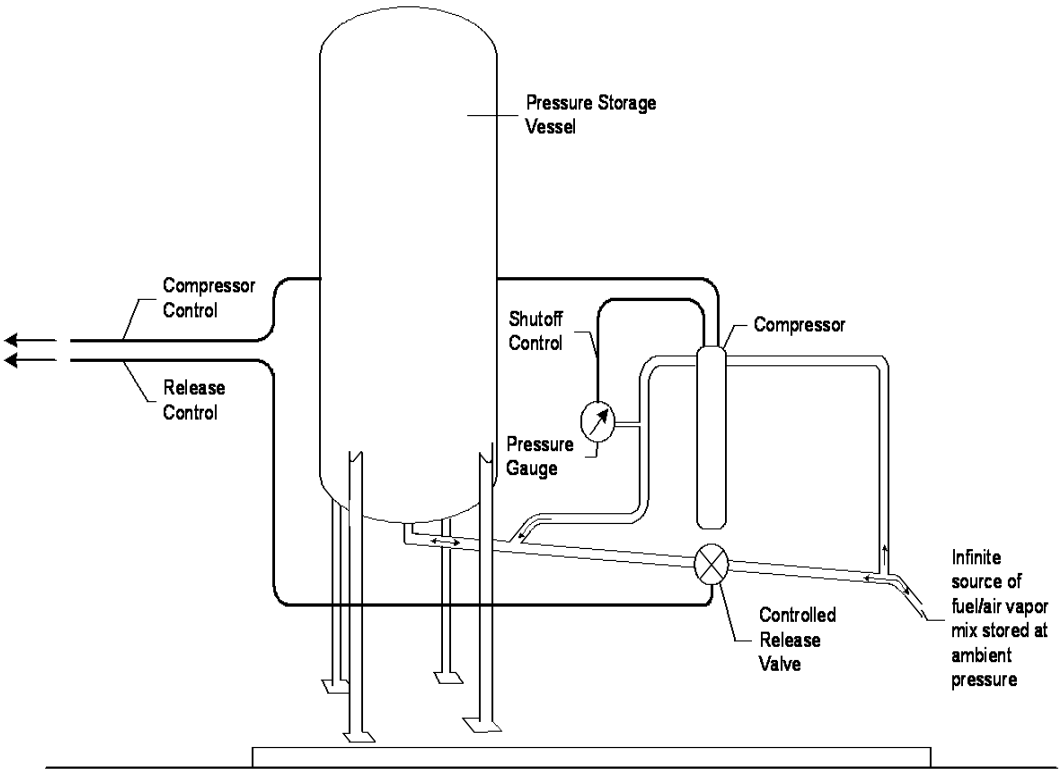

Figure 1: Schematic diagram of the system to be investigated

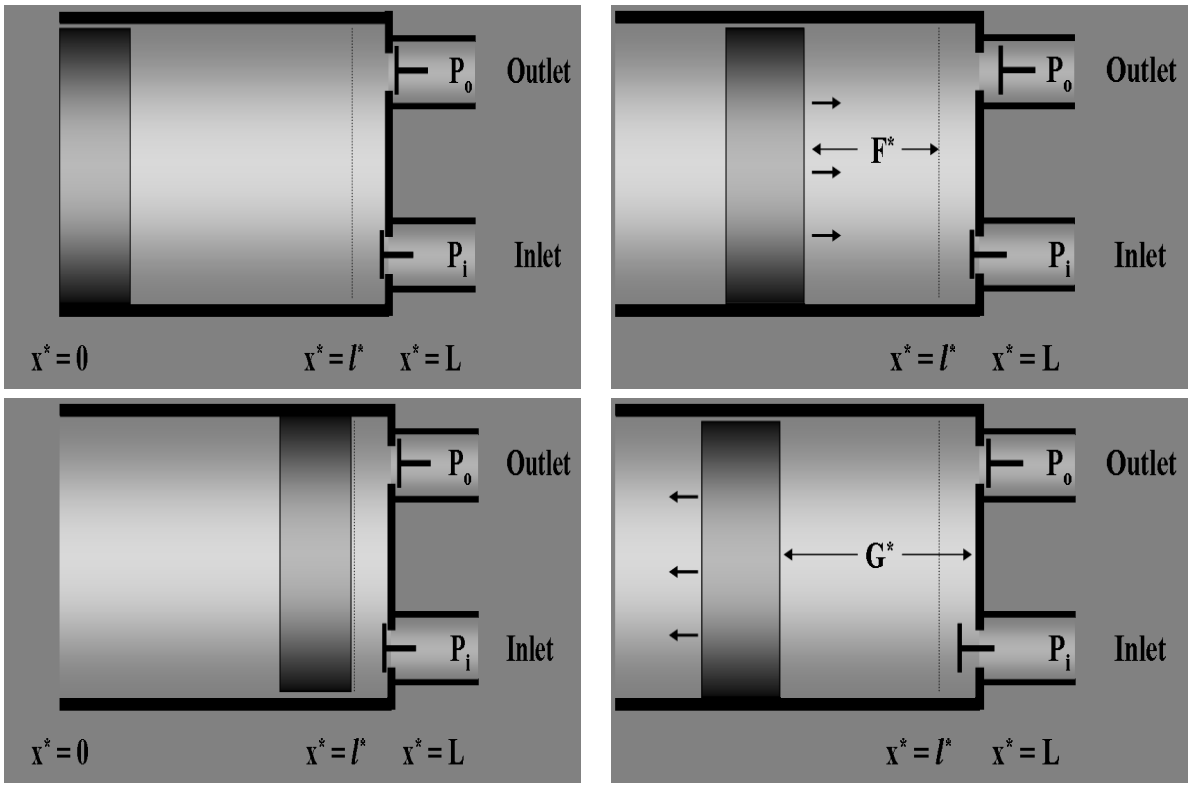

Figure 2: Representation of the four stages of the compression cycle. Top-left diagram: Stage 1, the vapor at ambient conditions initially is compressed to the storage-tank pressure; Top-right diagram: Stage 2, the exhaust valve now opens, and the vapor is discharged into the storage tank; Bottom-left diagram, Stage 3, the piston reverses direction, the exhaust valve closes, and the remaining vapor expands and cools until the ambient pressure is reached; Stage 4, the inlet valve opens, bringing fresh gas at ambient pressure into the tank to be compressed in the next cycle.

$$\rho^* \left\{ \mathbf{u}^*_{t^*} + \mathbf{u}^* \cdot \nabla \mathbf{u}^* \right\} + \nabla p^* = \mu \nabla^2 \mathbf{u}^* \tag{2}$$

$$\rho^* \, c_{vo} \left\{ T^*_{t^*} + \mathbf{u}^* \cdot \nabla T^* \right\} + p^* \left(\nabla \cdot \mathbf{u}^* \right) = k_o \nabla^2 T^* \tag{3}$$

$$p^* = R \rho^* \, T^* \ , \tag{4}$$

where ρ^* is the density of the mixture, $\mathbf{u}^* = (u^*, v^*)$ is the gas velocity (axial and radial components), p^* is the gas pressure, μ is the gas dynamic viscosity, c_{vo} is the specific heat of the gas at constant volume, T^* is the gas temperature, k_o is the thermal conductivity of the gas, and $R = c_{po} - c_{vo}$ is the universal gas constant. This system is coupled to the energy equation in the cylindrical shell:

$$\rho_w c_{pw} T_{w\, t^*} = k_w \nabla^2 T_w \ , \tag{5}$$

where ρ_w is the density of the material of the wall, c_{pw} is the specific heat at constant pressure in the wall, T_w is the wall temperature, and k_w is the thermal conductivity of the wall.

There are four cycle stages which correspond to the boundary data. In the top-left diagram in Figure 2 we see a representation of stage 1. During this stage, the gas is compressed, and both valves remain closed. When the pressure of the gas in the compressor is the same as the pressure in the external tank, then the exhaust valve opens, and the vapor is put into the external tank. This is the start of stage 2, shown in the top-right diagram of Figure 2, which begins when the piston is a distance $l^* + F^*$ from the compressor wall,

Material	Quantity	Units	Values
Air (at 300 K)	ρ_o	$\mathrm{kg/m^3}$	1.29
	c_{vo}	J/(kg K)	1000
	k_o	W /(m K)	0.025
	κ_o	$\mathrm{m^2/s}$	1.9×10^{-4}
Cast Aluminium (91.5% Al)	ρ_w	$\mathrm{kg/m^3}$	2800
	c_{pw}	J/(kg K)	2.4×10^{6}
	k_w	W/(m K)	150
	κ_w	$\mathrm{m^2/s}$	5×10^{-5}
	h	$\mathrm{W/(m^2\,K)}$	1 - 10
Design Quantity	**Variable**	**Units**	**Values**
Compressor Length	L	m	0.1
Piston Stroke	l^*	m	0.08-0.09
Piston Radius	a	m	0.025
Compression Casing Thickness	b	m	0.005
Piston Cross-sectional Area	A_p	$\mathrm{m^2}$	2.0×10^{-3}
Storage Tank Volume	V_s	$\mathrm{m^3}$	0.06
Piston Stroke Frequency	f	$\mathrm{s^{-1}}$	1
Characteristic Piston Velocity	U_p	m/s	0.1

Table 1: Dimensional material and design properties.

where F^* needs to be determined from the state of the gas. After the piston has reached $x^* = l^*$, stage 3 begins as the piston reverses direction. During this stage, the pressure drops below the pressure in the tank and both valves remain closed (see the bottom-left figure in Figure 2). When the pressure drops below the value in the intake tank, then the intake valve opens and a mixture at ambient conditions enters the tank. Stage 4, as shown in the bottom-right diagram of Figure 2, starts when the piston is a distance G^* from the compressor wall. This stage continues until the piston returns to the original position at the start of stage 1, at which point the cycle repeats.

Mathematically, these stages can be, in an ideal case, described as:

Stage 1: Compression. $t_o^* < t^* < t_1^*$

$$
\begin{aligned}
x^* = x_p^*(t^*): \quad & u^* = \frac{d}{dt^*} x_p^*(t^*)\ , v^* = 0 \\
& T_{x^*}^* = 0 \\
x^* = L: \quad & u^* = 0 \\
& v^* = 0 \\
& T_{x^*}^* = 0 \\
r^* = 0: \quad & r^*\, T_{r^*}^* = 0 \\
& v_r^* = 0 \\
r^* = a: \quad & T^* = T_w \\
& k_o\, r^*\, T_{r^*}^* = k_w\, r^*\, T_{wr^*}^* \\
& v^* = 0 \\
r^* = a + b: \quad & k_w\, T_{wr^*} = -h\,(T_{wr^*} - T_o)\ ,
\end{aligned}
$$

Stage 2: Isobaric Exhaust. $t_1^* < t^* < t_2^*$

$$
\begin{aligned}
x^* = x_p^*(t^*): \quad & u^* = \frac{d}{dt^*} x_p^*(t^*)\ , v^* = 0 \\
& T_{x^*}^* = 0 \\
x^* = L: \quad & v^* = 0 \\
& T_{x^*}^* = 0 \\
r^* = 0: \quad & r^*\, T_{r^*}^* = 0 \\
& v_r^* = 0 \\
r^* = a: \quad & T^* = T_w \\
& k_o\, r^*\, T_{r^*}^* = k_w\, r^*\, T_{wr^*}^* \\
& v^* = 0 \\
r^* = a + b: \quad & k_w\, T_{wr^*} = -h\,(T_{wr^*} - T_o)\ ,
\end{aligned}
$$

Stage 3: Expansion $t_2^* < t^* < t_3^*$

$$
\begin{aligned}
x^* = x_p^*(t^*): \quad & u^* = \frac{d}{dt^*} x_p^*(t^*)\ , v^* = 0 \\
& T_{x^*}^* = 0 \\
x^* = L: \quad & u^* = 0 \\
& v^* = 0 \\
& T_{x^*}^* = 0 \\
r^* = 0: \quad & r^*\, T_{r^*}^* = 0 \\
& v_r^* = 0 \\
r^* = a: \quad & T^* = T_w \\
& k_o\, r^*\, T_{r^*}^* = k_w\, r^*\, T_{wr^*}^* \\
& v^* = 0 \\
r^* = a + b: \quad & k_w\, T_{wr^*} = -h\,(T_{wr^*} - T_o)\ ,
\end{aligned}
$$

Stage 4: Isobaric Intake. $t_3^* < t^* < t_4^*$

$$
\begin{aligned}
x^* = x_p^*(t^*): \quad & u^* = \frac{d}{dt^*} x_p^*(t^*)\ , v^* = 0 \\
& T_{x^*}^* = 0 \\
x^* = L: \quad & v^* = 0 \\
& T_{x^*}^* = 0 \\
r^* = 0: \quad & r^*\, T_{r^*}^* = 0 \\
& v_r^* = 0 \\
r^* = a: \quad & T^* = T_w \\
& k_o\, r^*\, T_{r^*}^* = k_w\, r^*\, T_{wr^*}^* \\
& v^* = 0 \\
r^* = a + b: \quad & k_w\, T_{wr^*} = -h\,(T_{wr^*} - T_o)\ ,
\end{aligned}
$$

where h is the heat transfer coefficient between the cylindrical wall and the environment.

The critical problem to consider is the heat transport from the compressing vapor to its surroundings. With this, we shall focus on the heat transport aspects of this system, and not concern ourselves immediately with the fluid-mechanical details of the system. We perform a scaling analysis to justify these assumptions.

Scale x^* on L, r^* on a, t^* on $1/f$, where f is the frequency of the piston oscillation, $\mathbf{u}^*$ on $U_p = L\,f$, and gas properties on their ambient values ρ_o, p_o, T_o such that $p_o = R\rho_o T_o$. From this nondimensionalization, the resulting equations are in the gas $x_p(t) < x < 1, 0 < r < 1, t > 0$:

$$\rho_t + (\rho\,u)_x + \frac{L}{a}\,\frac{1}{r}(r\rho\,v)_r = 0 \tag{6}$$

$$\frac{\rho_o\,U_p^2}{p_o}\rho\left\{u_t + uu_x + \frac{L}{a}vu_r\right\} + p_x = \frac{\mu U_p}{p_o\,L}\left\{\frac{L^2}{a^2}\,\frac{1}{r}\,(ru_r)_r + u_{xx}\right\} \tag{7}$$

$$\frac{\rho_o\,U_p^2}{p_o}\rho\left\{v_t + uv_x + \frac{L}{a}vv_r\right\} + \frac{L}{a}\,p_r = \frac{\mu U_p}{p_o\,L}\left\{\frac{L^2}{a^2}\,\frac{1}{r}\,(rv_r)_r + v_{xx}\right\} \tag{8}$$

$$\rho\left\{T_t + uT_x + \frac{L}{a}\,vT_r\right\} + \frac{R}{c_{vo}}\,p\left(u_x + \frac{L}{a}\frac{1}{r}(rv)_r\right) = \frac{\kappa_o}{L\,U_p}\left\{\frac{L^2}{a^2}\,\frac{1}{r}\,(rT_r)_r + T_{xx}\right\} \tag{9}$$

$$p = \rho\,T\ , \tag{10}$$

where $\kappa_o = k_o/(\rho_o c_{vo})$ is the thermal diffusivity of the vapor.

In the cylindrical shell, we have that

$$T_{wt} = \frac{\kappa_w}{L\,U_p}\left\{\frac{L^2}{a^2}\,\frac{1}{r}\,(rT_{wr})_r + T_{wxx}\right\}\ , \tag{11}$$

where $\kappa_w = k_w/(\rho_w c_{pw})$ is the thermal diffusivity of the wall material. The boundary conditions then become (only Stage 1 is shown below):

$$\begin{aligned}
x = x_p(t):&\quad u = x_p'(t)\ , v = 0\\
&\quad T_x = 0\\
x = 1:&\quad u = 0\\
&\quad v = 0\\
&\quad T_x = 0\\
r = 0:&\quad r\,T_r = 0\ ,\ v_r = 0\\
r = 1:&\quad T = T_w\\
&\quad \frac{k_o}{k_w}r\,T_r = r\,T_{wr}\\
&\quad v = 0\\
r = 1 + \frac{b}{a}:&\quad T_{wr} = -\frac{h\,a}{k_w}\,(T_w - 1)
\end{aligned}$$

Note that for the system at hand, $U_p^2\rho_o/p_o \approx 10^{-8}$, $\mu U_p/(Lp_o) \approx 10^{-10}$, $L/a \approx 10$, and $\kappa/(LU_p) \approx 10^{-3}$. Further, for cast aluminum, we find that $\kappa_w/(LU_p) \approx 10^{-3}$. Thus, both momentum equations to leading order give us that $p_x = p_r = 0$, or that $p = p(t)$, and further requires us to not solve for one of the dependent variables. The leading-order effect in the conservation of mass equation gives

$$r\rho v = A\ \ ,$$

and since $v = 0$ on $r = 1$, $A = 0$. Since $\rho \neq 0$ by the equation of state, we have that $v = 0$. The resulting equations then become:

$$\rho_t + (\rho\,u)_x = 0 \tag{12}$$

$$p_x = 0 \tag{13}$$

$$\rho\,\{T_t + uT_x\} + (\gamma - 1)\,p\,u_x = \lambda_o\left\{\frac{1}{r}\,(rT_r)_r + \epsilon^2 T_{xx}\right\} \tag{14}$$

$$p = \rho\,T\ , \tag{15}$$

Quantity Name	Variable	Typical Values
Mach Number Squared	$M^2 = \left(\frac{\rho_o U_p^2}{p_o}\right)^2$	10^{-8}
Viscous Term	$\frac{\mu U_p}{L\, p_o}$	10^{-10}
Specific Heat Ratio	γ	1.4
Vapor Thermal Diffusion	λ_o	0.3
Aspect Ratio	ϵ	0.1
Volume Ratio	$V = (LA_p/V_s)$	3×10^{-3}
Scaled Wall Thickness	$d = b/a$	0.2
Wall Thermal Diffusion	λ_w	0.08
Thermal Conductivity Ratio	K	2×10^{-4}
Biot Number (heat transfer)	B	8×10^{-4}

Table 2: Dimensionless quantities and their typical values

where $\epsilon = a/L$ is the aspect ratio of the compressor, and $\lambda_o = (L\kappa_o)/(a^2\, U_p)$ is the ratio of the rate of heat propagation to advection. This, along with the heat equation in the wall:

$$T_{wt} \quad = \quad \lambda_w \left\{ \frac{1}{r} \left(r T_{wr} \right)_r + \epsilon^2 T_{wxx} \right\} \ , \tag{16}$$

where $\lambda_w = (L\kappa_w)/(a^2\, U_p)$ is the ratio of heat transport through the cylinder to advection.

The boundary conditions for this system are (again, only Stage 1 is shown here):

$$x = x_p(t): \qquad u = x_p'(t)\ , T_x = 0 \tag{17}$$

$$x = 1: \qquad u = 0 \tag{18}$$

$$T_x = 0 \tag{19}$$

$$r = 0: \qquad r\, T_r = 0 \tag{20}$$

$$r = 1: \qquad T = T_w \tag{21}$$

$$K\, r\, T_r = r\, T_{wr} \tag{22}$$

$$r = 1 + d: \qquad T_{wr} = -B\, (T_w - 1) \tag{23}$$

where $K = k_o/k_w \approx 10^{-4}$ is the ratio of thermal conductivities of the wall material to the vapor, $B = h\, a/k_w \approx 10^{-3}$ is the Biot number, and $d = b/a$ is the relative thickness of the apparatus casing to its radius.

3 Results

3.1 Perfectly Insulated System

The simplest case of the system (12) - (16) subject to the boundary conditions (17)-(23), during all four stages, is to assume that there is no heat transport out of the chamber. Hence, if $\lambda_o = \lambda_w = B = K = 0$, then there is no net heat flux through the side walls, resulting in the following set of equations:

$$\begin{aligned} \rho_t + (\rho\, u)_x &= 0 \\ p_x &= 0 \\ \rho T_t + (\gamma - 1)\, p u_x &= 0 \\ p &= \rho T\ . \end{aligned}$$

Note that for $\gamma = 1$, we recover the isothermal case, again ignoring the effects of the chamber on the compression process. We shall include this case in the results below.

We identify the boundary conditions that occur at each stage:

Stage 1:

$$t_o < t < t_1 : \quad u(x_p(t), t) = x_p'(t), u(1, t) = 0 \ , \tag{24}$$

Stage 2:

$$t_1 < t < t_2 : \quad u(x_p(t), t) = x_p'(t) \ , \tag{25}$$

Stage 3:

$$t_2 < t < t_3 : \quad u(x_p(t), t) = x_p'(t), u(1, t) = 0 \ , \tag{26}$$

Stage 4:

$$t_3 < t < t_4 : \quad u(x_p(t), t) = x_p'(t) \ , \tag{27}$$

Note that the times t_1, t_3 are determined implicitly by $p(t_1) = P_s^{(n)}$, $p(t_3) = 1$, where $P_s^{(n)}$ is the pressure within the storage tank during cycle n. We are going to find how the pressure in the tank increases from one cycle to the next through the compression process.

During stage 1, $u(x_p(t), t) = x_p'(t)$, $u(1, t) = 0$. We can solve for the velocity u from the conservation of mass relation

$$u = -\frac{\rho_t}{\rho} (x - 1) \ ,$$

and the velocity condition at the piston results in

$$\rho(t) = \frac{1}{1 - x_p(t)} \ .$$

Using this information and the equation of state, the energy equation becomes

$$\rho T_t - (\gamma - 1) \rho_t T = 0 \ ,$$

or that

$$T(t) = \rho^{\gamma - 1} \ .$$

This with the equation of state results in the standard adiabatic solution

$$p(t) = \rho^{\gamma} \ .$$

At time $t = t_1$, $p(t) = P_s^{(n)}$, $u(x, t) = x_p'(t)$ identically, and the density and temperature do not change during this stage. We define the following quantities at this time:

$$F^{(n)} = 1 - l - x_p(t_1) \tag{28}$$

$$T^{(n)} = T(t_1) \tag{29}$$

$$\rho^{(n)} = \rho(t_1) \ . \tag{30}$$

At time $t = t_2$, the additional mass added to the storage tank is given by $M^{(n)} = \rho^{(n)} F^{(n)} V$, where $V = (L A_p / V_s)$ is the ratio of the volume in the compressor to that within the storage tank.. With this added mass, we can calculate what the new storage tank pressure, which is under isothermal conditions:

$$P_s^{(n+1)} = P_s^{(n)} + V \rho^{(n)} F^{(n)} \ .$$

During Stage 3, the gas expands, and the solution to the pressure, density and temperature are given by

$$\rho(t) = \frac{\rho^{(n)} (1 - l)}{1 - x_p(t)} \ , \ T(t) = \rho^{\gamma - 1} \ , \ p(t) = \rho^{\gamma} \ . \tag{31}$$

Lastly, during Stage 4, the input valve opens, and ambient material enters the system, giving that $\rho = 1, p = 1, T = 1$.

To find how the pressure in the storage tank increases, we recall that the exhaust valve opens when $p(t_1) = P_s^{(n)}$. This gives a relation between $F^{(n)}, \rho^{(n)}$, and $P_s^{(n)}$:

$$\begin{aligned} p(t_1) &= P_s^{(n)} \\ &= (\rho(t_1))^\gamma = \left(\rho^{(n)}\right)^\gamma \\ \Rightarrow \qquad \rho^{(n)} &= \left(P_s^{(n)}\right)^{(1/\gamma)} \ , \end{aligned}$$

and at $t = t_1$:

$$\begin{aligned} \rho(t_1) = \rho^{(n)} &= \frac{1}{1 - x_p(t_1)} \\ &= \frac{1}{1 - l - F^{(n)}} \end{aligned}$$

or

$$F^{(n)} = \left(\frac{1}{P_s^{(n)}}\right)^{1/\gamma} - (1 - l) \ .$$

Hence, our first-order difference system for the storage-tank pressure is given by

$$P_s^{(n+1)} = P_s^{(n)} + V \left\{1 - (1 - l)\left[P_s^{(n)}\right]^{1/\gamma}\right\} \ . \tag{32}$$

In Figure 3 we show the trajectory of the storage tank pressure $P_s^{(n)}$ over a typical filling process plotted against the cycle n for various γ from isothermal ($\gamma = 1$) to the adiabatic case for air $\gamma = 1.4$. In the actual application, which contains a mixture of primarily n-Butane (C_4H_{10}), Pentane (C_5H_{12}) and Hexane (C_6H_{14}) at a volume fraction of about 20%, a weighted average for the specific heat ratio gives $\gamma \approx 1.3$. In the lower figure, we plot the temperature $T^{(n)}$ at the beginning of the exhaust stage for the n^{th} cycle. Notice that for the mixture in question that the final temperature at a 10-fold compression is approximately 530 K. This final temperature is near the auto-ignition point of the mixture, which is not desirable for stable operating conditions.

3.2 Effect of the Compressor Walls

The previous analysis assumed that there was no heat transfer to or from the system. However, the time scale on which the storage tank fills (approximately 10,000 s) is comparable to the typical time scale of heat transfer through the compressor walls and out to the environment. Since these effects occur on the same time scale, their competition is important to understand.

We start with equations (12)-(15), multiply each equation by r and integrate over $0 < r < 1$ to arrive at the following system of equations, where ρ, u, p and T are assume to be averaged values in r:

$$\rho_t + (\rho\, u)_x = 0 \tag{33}$$

$$p_x = 0 \tag{34}$$

$$\rho\ \{T_t + uT_x\} + (\gamma - 1)\ p\, u_x = \lambda_o \left\{2\, Q + \epsilon^2 T_{xx}\right\} \tag{35}$$

$$p = \rho T \ , \tag{36}$$

where $Q = rT_r|_{r=1}$ is a measure of the amount of heat transfer that occurs between the vapor in the compressor and the compressor walls. We have assumed that the spatial dependence of ρ, u_x, p, T is not significant in the majority of the compression chamber, and that only the heat flux through the chamber

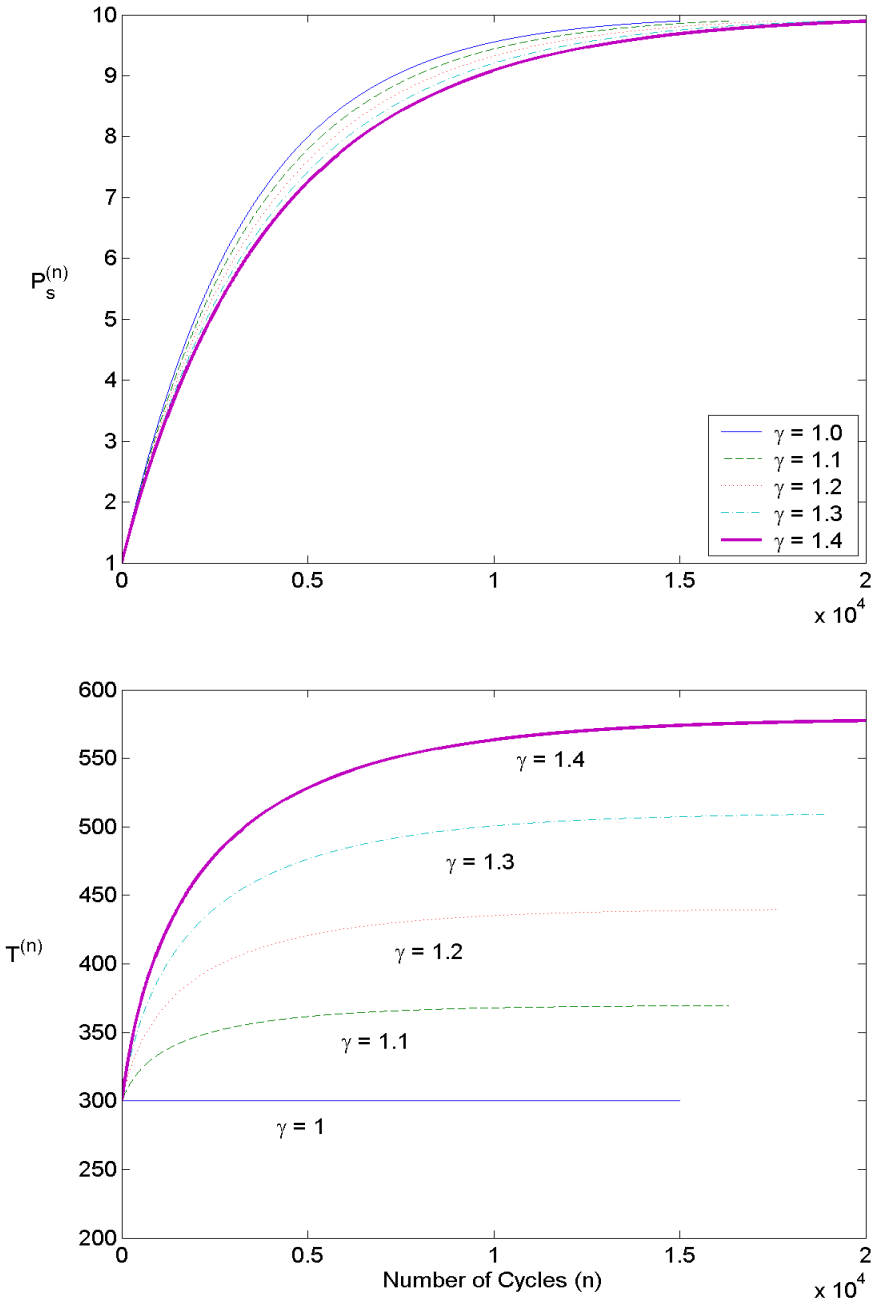

Figure 3: Pressure and Temperature rise for the adiabatic case, independent of wall temperatures, for $\gamma = 1$, $\gamma = 1.1$, $\gamma = 1.2$, $\gamma = 1.3$, and $\gamma = 1.4$ with $l = (0.1)^\gamma$ and $V = 0.003$. For a 20% mixture of n-Butane, Pentane, and Hexane with dry air ($\gamma \approx 1.3$), the final temperature reaches approximately 530 K.

walls is the only significant effect. Thus, all of the dependent variables can be represented as functions of time.

The average temperature of the cylinder wall, $\bar{T}_w = \int_1^{1+d} r T_w \, dr$, varies slowly in time. We can see this by multiplying the heat equation within the cylinder walls by r and integrating over this domain to find that

$$\frac{\partial \bar{T}_w}{\partial t} = \frac{2\,\lambda_w}{2d+d^2}\left\{-B[T_w(1,t)-1] - K\,Q(t)\right\} \quad . \tag{37}$$

Since $B, K = O(V) \approx 10^{-3}$, the average wall temperature within the cylinder changes slowly over time t. For the following, we make the approximation that $T_w(1,t) \approx \bar{T}_w$, and if we integrate (37) over one cycle in time, then we can write

$$T_w^{(n+1)} - T_w^{(n)} = -\frac{2\,\lambda_w}{2d+d^2}\left\{B\left[T_w^{(n)} - 1\right] + KQ^{(n)}\right\} \ , \tag{38}$$

where we have approximated the average temperature in t of $\bar{T}_w$ with $T_w^{(n)}$ and the average value of the heat flux as $Q^{(n)}$.

In the following, we need an additional relation to determine the heat flux across the interior chamber wall. We consider only two cases here. The first is to assume that the average wall temperature, through the continuity of temperature condition and a uniform gas temperature T in space, is the same as the average vapor temperature T over this cycle. This additional condition provides a constraint for the heat Q, and if we assume that the value of Q does not vary significantly over one cycle, closes the system. This is a quasi-steady assumption on the heat flux, and is the simplest system to analyze.

A second approach is to assume that the heat flow is related to the temperature of the vapor and the wall through a Newton's law of cooling approach $Q = -\alpha(T - T_w)$, where α is the heat transfer parameter from the wall to the vapor, and would need to be determined by experiment. Again, the vapor system needs to be determined during each cycle, and the resulting analysis needs to be coupled to the wall temperature through (38). Notice that T_w in this analysis is quasi-steady by (37).

In both approaches, a system of discrete equations is derived that describes the wall and vapor temperature at each cycle n.

3.2.1 Maximum wall temperature near the end of the process

On the long time scale of thousands of pump cycles, the temperature of the pump walls near the inlet/outlet end will increase due to the heat of compression of the gas; once this occurs, the hot walls heat the gas prior to compression creating a feedback loop. As a worst case, let us assume that the walls near the inlet/outlet $x = 1$ reach a maximum temperature of the gas T_M, and let us attempt to estimate (or find an upper bound for) this temperature. We assume that the gas is sufficiently well-mixed to prevent the formation of a boundary layer near the walls, which is not ideal, but is crucial in the following calculation.

Late in the process, the region $l < x < 1$ along the cylindrical portion of the walls and the end-wall will attain this temperature T_M. This localized region, assuming that the heat capacity of the compressor walls is much larger than that of the gas, provides a source of heat during the intake cycle. Assuming that the piston moves at a constant speed $x'(t) = \pm 1$, then the energy equation for the gas is given by

$$\rho T_t \quad = \quad \alpha\,(T_M - T) \ , \tag{39}$$

where

$$\alpha = \left(\frac{2}{a} + \frac{1}{L(1-l)}\right)\frac{h_C}{c_{vo}\rho_o} \ ,$$

where h_C is the heat transfer coefficient between the gas and the compressor walls, which needs to be determined experimentally. In the following, we assume initially that the density of the gas remains constant during the intake process. We shall compare this result to that for a constant pressure intake later in this subsection.

The intake phase lasts a duration $1-G$, where $G=(1-l)\,p_s^{1/\gamma}$ in the adiabatic case, and hence the temperature at the end of this phase T_4 is given by

$$(T_M - T_4) = (T_M - 1)\exp\left\{-\alpha(1-G)\right\} \ .$$

The intake phase is followed by the compression phase. If the compression is adiabatic from $p=1$ to $p=p_s$ and that the temperature rises back to T_M, one finds that

$$T_4 = T_M p_s^{\frac{1-\gamma}{\gamma}} \ .$$

Combining the previous two equations, one obtains an explicit formula for T_M (using the adiabatic form of G):

$$T_M \quad = \quad \left[1-(1-p_s^{\frac{1-\gamma}{\gamma}})\exp\left\{\alpha(1-(1-l)p_s^{1/\gamma})\right\}\right]^{-1} \ . \tag{40}$$

A similar analysis, assuming that the intake process is isobaric ($\rho = 1/T$) yields the following expression between $T_M$and T_4:

$$T_M - 1 \quad = \quad \frac{T_M\,(T_M-T_4)\,e^{\alpha T_M(1-G)}}{(T_M-T_4)e^{\alpha T_M(1-G)}+T_4} \ . \tag{41}$$

Applying an adiabatic compression phase (3.2.1) results in the relation

$$T_M - 1 \quad = \quad T_M\left\{\frac{(1-p_s^{\frac{1-\gamma}{\gamma}})e^{\alpha T_M(1-G)}}{(1-p_s^{\frac{1-\gamma}{\gamma}})e^{\alpha T_M(1-G)}+p_s^{\frac{1-\gamma}{\gamma}}}\right\} \ , \tag{42}$$

which simplifies to

$$T_M = \left[(p_s^{\frac{1-\gamma}{\gamma}}-1)\exp\left\{-\alpha\,T_M\,(1-G)\right\}\ +1\right] \ .$$

In figure 4, we show in the results for $\alpha = 0.125, 0.25$ and 0.5, $l=0.9$, and using the adiabatic result for the distance G at which the intake valves open. The upper figure corresponds to the isochoric case, while the lower figure corresponds to the isobaric case. Notice that in the isochoric regime, the bounds on the maximum temperature (assuming that the compressor wall reaches a steady-state maximum temperature) is larger than that of the adiabatic temperature (solid curve). However, in the isobaric case, the maximum possible temperature is actually *cooler* than the isochoric case. This can be understood easily, since the density *increases* during this stage. The equation of state then suggests that, since pressure is constant, the temperature decreases during this stage.

3.2.2 Quasi-steady Q

The following analysis is the easiest case to solve (33)-(36) with (38). It is an interesting case to consider next to the more realistic case of the heat flux being proportional to the temperature difference between the gas and the chamber wall.

Note that with the assumptions that we have made, we can solve for T in equation (35) directly with

$$T = T_i\left(\frac{\rho}{\rho_i}\right)^{\gamma-1} + 2\,\lambda_o\,\rho^{\gamma-1}\int_{t_i}^{t} Q\,\rho^{-\gamma}\,d\bar{t} \ , \tag{43}$$

where the i subscript corresponds to the values at the beginning at that stage. In the following isobaric conditions (pressure is constant) are assumed whenever a valve is opened. Further, we assume that the piston speed is constant (either ± 1), and hence we can relate piston position directly with time. This assumption is convenient for the averaging process.

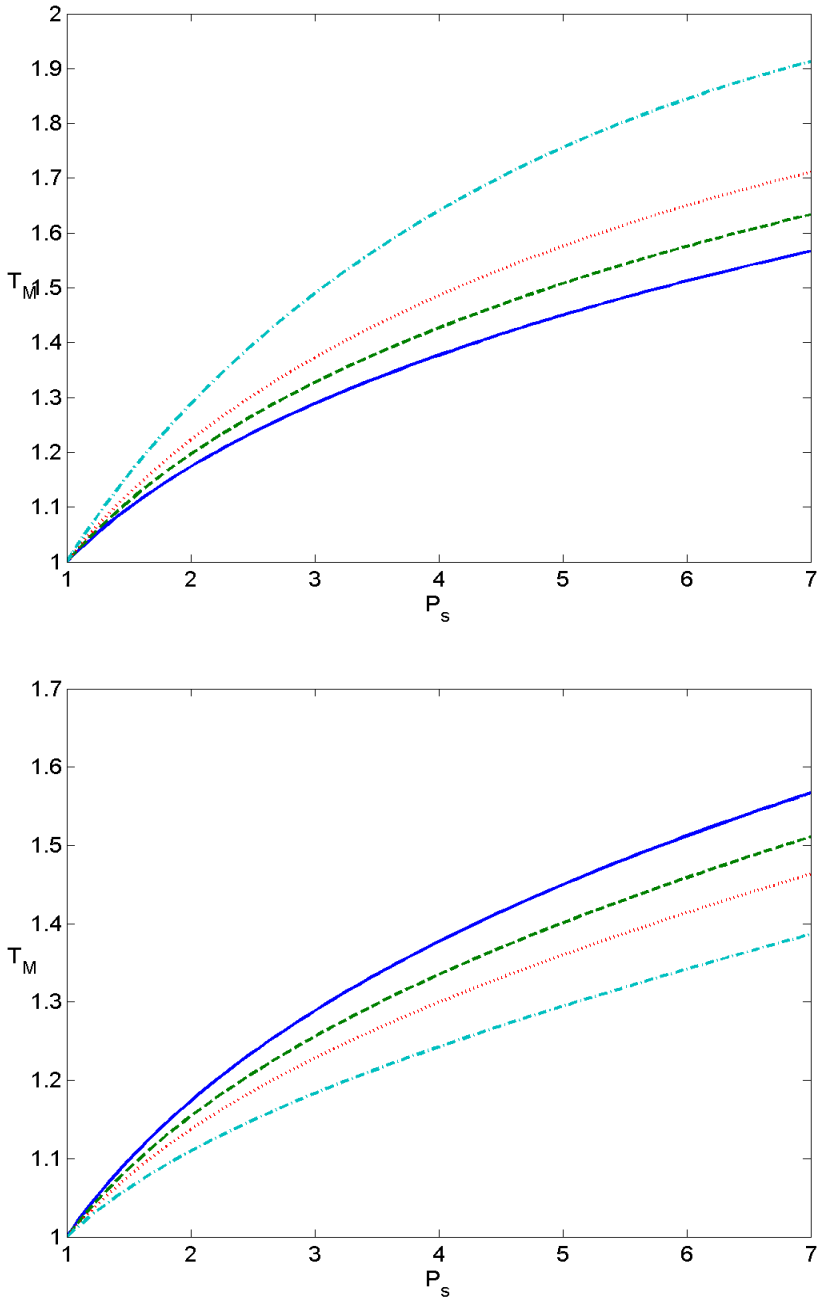

Figure 4: Comparison of the maximum temperature calculations for the isochoric intake case (upper figure) and the isobaric intake case (lower figure). In both cases, the solid curve corresponds to the adiabatic limit ($\alpha = 0$), while the dashed curve, dotted curve, and dashed-dotted curves correspond to $\alpha = 0.125, 0.25$, and 0.5 respectively. Notice that in the isochoric case, if the maximum temperature does exist, it may be higher than the adiabatic temperature. However, in the isobaric case, the maximum temperature, if it exists, can be lower than the adiabatic case.

During stage 1, both valves are closed, and the density and temperature are given by

$$\rho = \frac{\rho_o}{1 - x_p(t)} \ , t_o < t < t_1 \ ,$$

and the form of the temperature in this region is given by (43). This formulation is valid up until $t = t_1$, when the pressure $p(t_1) = P_s^{(n)}$. At this time, $x_p(t_1) = l - F^{(n)}$, which gives a relation between $F^{(n)}$ and $P_s^{(n)}$:

$$P_s^{(n)} = \left[p_o + \frac{2\,\lambda_o\,Q^{(n)}}{\gamma + 1} \right] \left[\frac{1}{1 - l + F^{(n)}} \right]^{\gamma} - \frac{2\,\lambda_o\,Q^{(n)}}{\gamma + 1} \left[1 - l + F^{(n)} \right] \ . \tag{44}$$

During stage 2, $t_1 < t < t_2 = t_o + 1/2$, $p(t) = P_s^{(n)}$, which gives us an equation for the density ρ:

$$P_s^{(n)} = \rho_1 T_1 \left(\frac{\rho}{\rho_1} \right)^{\gamma} + 2\,\lambda_o\,Q \rho^{\gamma} \int_{t_1}^{t} \rho^{-\gamma} d\bar{t} = \rho T \ . \tag{45}$$

Differentiating (45) once with respect to t gives an ordinary differential equation to solve for ρ:

$$\rho'(t) = -\frac{2\,\lambda_o\,Q^{(n)}}{\gamma\,P_s^{(n)}}\,\rho \ ,$$

results in the following equations for the density and temperature during stage 2:

$$\rho(t) = \rho_1 e^{-\frac{2\lambda_o\,Q^{(n)}}{\gamma P_s^{(n)}}\,(t - t_1)} \ , \ T(t) = \frac{P_s^{(n)}}{\rho_1} e^{\frac{2\lambda_o\,Q^{(n)}}{\gamma P_s^{(n)}}(t - t_1)} \ . \tag{46}$$

Note that this results in the velocity u not being uniform over x,

$$u = x_p'(t) + \frac{2\lambda_o\,Q^{(n)}}{\gamma P_s^{(n)}} \left[x - x_p(t) \right] \ . \tag{47}$$

.

Hence, the total mass $M^{(n)}$ that is put into the storage tank during this compression cycle is given by

$$\begin{aligned} M^{(n)} &= \int_{t_1}^{t_2} \rho(t) u(1,t) dt \\ &= \int_{t_1}^{t_2} \left[\rho x_p(t) \right]' - \rho'(t) dt \\ &= \rho^{(n)} \left\{ F^{(n)} + (l - 1) \left[e^{-\frac{2\,\lambda_o Q}{\gamma P_s^{(n)}}\,F^{(n)}} - 1 \right] \right\} \ , \end{aligned}$$

where $\rho^{(n)} = \rho_1$. Given that the time increase in the storage tank pressure is given by $\Delta P_s^{(n)} = V\,M^{(n)}$, we have that

$$P_s^{(n+1)} = P_s^{(n)} + V\,\rho^{(n)} \left\{ F^{(n)} + (l - 1) \left[e^{-\frac{2\,\lambda_o Q^{(n)}}{\gamma P_s^{(n)}}\,F^{(n)}} - 1 \right] \right\} \ . \tag{48}$$

Finally, the density and temperature at the end of this stage is given by

$$\rho_2 = \rho(t_2) = \rho_1 e^{-\frac{2\,\lambda_o\,Q^{(n)}}{\gamma P_s^{(n)}}\,F^{(n)}} \ , \ T_2 = T(t_2) = T_1 e^{\frac{2\,\lambda_o\,Q}{\gamma P_s^{(n)}}\,F^{(n)}} \ .$$

Stage 3, $t_2 < t < t_3$, is where some care must be shown. Since the thermodynamic process is not reversible here, we need to quantify how far the piston moves toward $x = 0$ while both valves remain closed.

We denote the location $x_p(t_3) = 1 - G^{(n)}$, where $G^{(n)}$ needs to be determined by the condition $p(t_3) = p_o$. The analysis is similar to Stage 1, and we find the equation for $G^{(n)}$ to be given by

$$p_o = P_s^{(n)} \left[\frac{1-l}{G^{(n)}}\right]^{\gamma} + \frac{2\,\lambda_o\,Q^{(n)}}{\left(G^{(n)}\right)^{\gamma}} \left\{\frac{\left(G^{(n)}\right)^{\gamma+1} - (1-l)^{\gamma+1}}{\gamma+1}\right\} , \tag{49}$$

and the resulting temperature field becomes

$$T(t) = T_2 \left(\frac{\rho}{\rho_2}\right)^{-1} \gamma + 2\,\lambda_o\,Q^{(n)} \rho^{\gamma-1} \int_{t_2}^{t} \rho^{-\gamma}\, d\bar{t} \, . \tag{50}$$

Finally, during stage 4, $p(t) = p_o$, and the density is governed by this isobaric condition, as in stage 2, and we find for the density and the temperature that

$$\rho = \rho_3 e^{-\frac{2\,\lambda_o\,Q^{(n)}}{\gamma p_o}(t-t_3)} \ , \ T(t) = \frac{p_o}{\rho_3} e^{\frac{2\,\lambda_o\,Q^{(n)}}{\gamma p_o}(t-t_3)} \ . \tag{51}$$

Lastly, we need to integrate this temperature $T(t)$ over the period $t_o < t < t_4 = t_o + 1$. Performing this integration,using the relations above, gives the result that over one period

$$\begin{aligned} T_w^{(n)} \;=\; & \frac{1}{2-\gamma} + \frac{2\lambda_o\,Q^{(n)}}{3\,p_o\,(\gamma+1)} \left[1-l+F^{(n)}\right]^3 - \frac{1}{2-\gamma}\left(1-l+F^{(n)}\right)^{2-\gamma} \left\{1 + \frac{2\lambda_o\,Q^{(n)}}{p_o}\right\} + \\ & \frac{\gamma\left(P_s^{(n)}\right)^2}{2\lambda_o\,Q^{(n)}\,p_o} \left(1-l+F^{(n)}\right) \left[e^{\frac{2\lambda_o\,Q^{(n)}}{\gamma P_s^{(n)}}\,F^{(n)}} - 1\right] + \\ & \left\{\frac{(1-l)^{\gamma}\left[\left(G^{(n)}\right)^{2-\gamma} - (1-l)^{2-\gamma}\right]}{2-\gamma} \left[1 + \frac{2\lambda_o\,Q^{(n)}}{(\gamma+1)\,P_s^{(n)}}\right] + \right. \\ & \left. \frac{2\lambda_o\,Q^{(n)}}{3(1-l)(\gamma+1)P_s^{(n)}} \left\{\left(G^{(n)}\right)^3 - (1-l)^3\right\}\right\} \left[1-l+F^{(n)}\right] \frac{P_s^{(n)}}{p_o} e^{-\frac{2\lambda_o\,Q^{(n)}}{\gamma P_s^{(n)}}\,F^{(n)}} + \\ & \frac{\gamma p_o G^{(n)}}{2(1-l)\lambda_o\,Q^{(n)}} \left[e^{\frac{2\lambda_o\,Q^{(n)}}{\gamma p_o}(1-G^{(n)})} - 1\right] \left[1-l+F^{(n)}\right] e^{-\frac{2\lambda_o\,Q^{(n)}}{\gamma P_s^{(n)}}\,F^{(n)}} \, . \end{aligned} \tag{52}$$

Thus, the system of equations in $T_w^{(n+1)}, P_s^{(n+1)}, F^{(n)}, G^{(n)}, Q^{(n)}$ which we need to solve is given by (52) and:

$$T_w^{(n+1)} - T_w^{(n)} \;=\; -\frac{2\,\lambda_w}{2d+d^2}\left\{B\left[T_w^{(n)} - 1\right] + KQ^{(n)}\right\} \tag{53}$$

$$P_s^{(n+1)} \;=\; P_s^{(n)} + V\,\rho^{(n)} \left\{F^{(n)} + (l-1)\left[e^{-\frac{2\,\lambda_o Q^{(n)}}{\gamma P_s^{(n)}}\,F^{(n)}} - 1\right]\right\} \tag{54}$$

$$P_s^{(n)} \;=\; \left[p_o + \frac{2\,\lambda_o\,Q^{(n)}}{\gamma+1}\right]\left[\frac{1}{1-l+F^{(n)}}\right]^{\gamma} - \frac{2\,\lambda_o\,Q^{(n)}}{\gamma+1}\left[1-l+F^{(n)}\right] \tag{55}$$

$$p_o \;=\; P_s^{(n)} \left[\frac{1-l}{G^{(n)}}\right]^{\gamma} + \frac{2\,\lambda_o\,Q^{(n)}}{\left(G^{(n)}\right)^{\gamma}} \left\{\frac{\left(G^{(n)}\right)^{\gamma+1} - (1-l)^{\gamma+1}}{\gamma+1}\right\} \tag{56}$$

$$\rho^{(n+1)} \;=\; \frac{\rho^{(n)}(1-l)}{(1-l+F^{(n+1)})G^{(n)}}\; e^{-\frac{2\,\lambda_o\,Q^{(n)}}{\gamma}\left[\frac{F^{(n)}}{P_s^{(n)}} + \frac{(1-G^{(n)})}{p_o}\right]} \tag{57}$$

A sample calculation of this system is shown in Figure 5 for larger Biot numbers ($B = 0.0008$)[1]. The storage-tank pressure, the wall temperature, and the relative piston locations when the exhaust and inlet

[1]Note that the solution to this system was found by converting it to a differential-algebraic system, and using the Matlab solver `ode15s` on this effective system

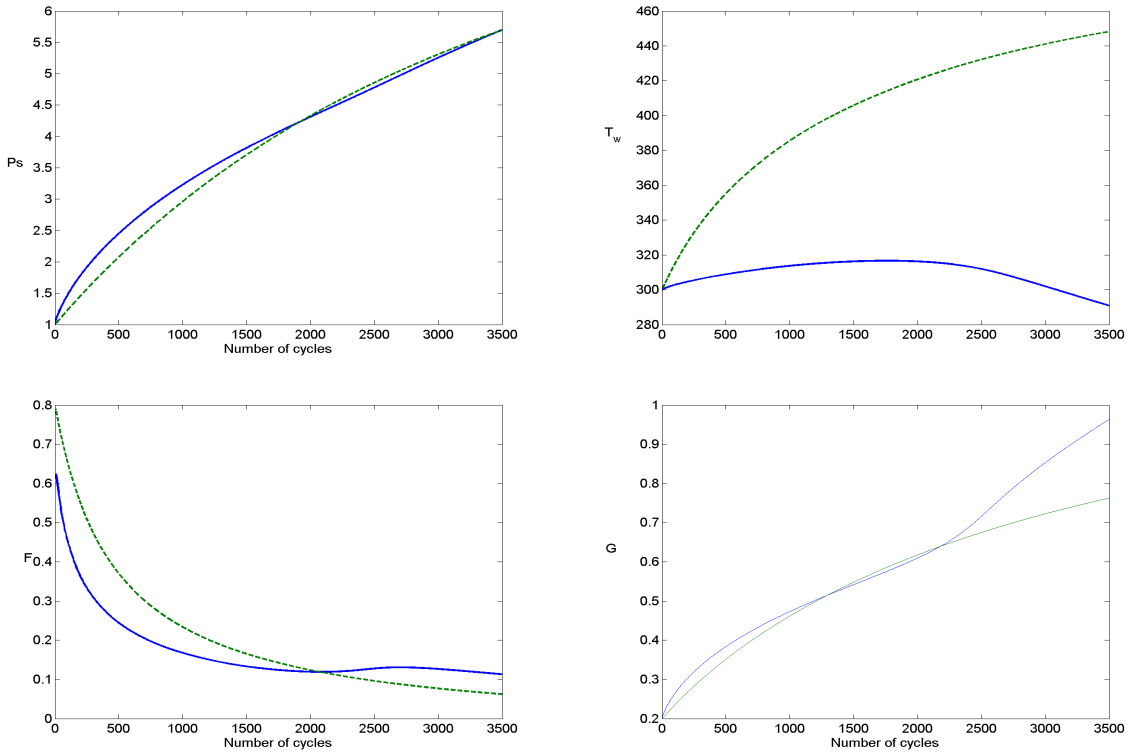

Figure 5: Storage-tank pressure, wall temperature, and piston positions F and G for a quasi-steady heat flux Q (solid line), plotted against the adiabatic result (dotted line) with $B = 0.0008$. Notice that the compressor continues operation longer than the adiabatic case, but eventually returns to the original temperature. At the end of the process, the input valves stop opening.

valves open, F and G respectively, are shown with solid curves while the dashed curves correspond to the adiabatic case (no heat flow from the vapor to the wall). Notice that the system ceases to function beyond around 3500 cycles, at which point $G = 1$ and the intake valve no longer opens. This results in a terminal pressure of about 6 atm. However, the effect of the heat transfer is apparent in the wall temperature, which never exceeds 320 K during this entire process. Note that the value of the Biot number is exceeding large in this example.

When the Biot number is smaller, however, we find that the compressor fails due to overheating. In Figure 6 we see the case for $B = 0.00008$. Notice that the storage-tank pressure peaks around 3 atm, the wall temperature starts to exceed the adiabatic temperature rise, and with $F = 0$, the exhaust valve ceases to open. Given the auto-ignition point of the vapor mixture, the mixture would combust within 3000 cycles.

3.2.3 Newton's Law: $Q = -\alpha(T - T_w)$

When the heat flux Q is assumed to depend on the vapor temperature, then the solution of the temperature, in terms of the density, is given by

$$T(t) = \left(\frac{\rho}{\rho_i}\right)^{\gamma-1} T_i e^{\int_{t_i}^{t} \frac{2\lambda_o \alpha}{\rho} d\bar{t}} + \rho^{\gamma-1} \int_{t_i}^{t} 2\lambda_o \alpha T_w^{(n)} \rho^{-\gamma} e^{\int_{\bar{t}}^{t} \frac{2\lambda_o \alpha}{\rho} d\tau} d\bar{t} \, .$$

Notice that the evolution of the vapor temperature is determined by the evolution of the density. From this basic solution for the vapor temperature, and assuming that $x_p'(t) = \pm 1$, we can follow the same process in the

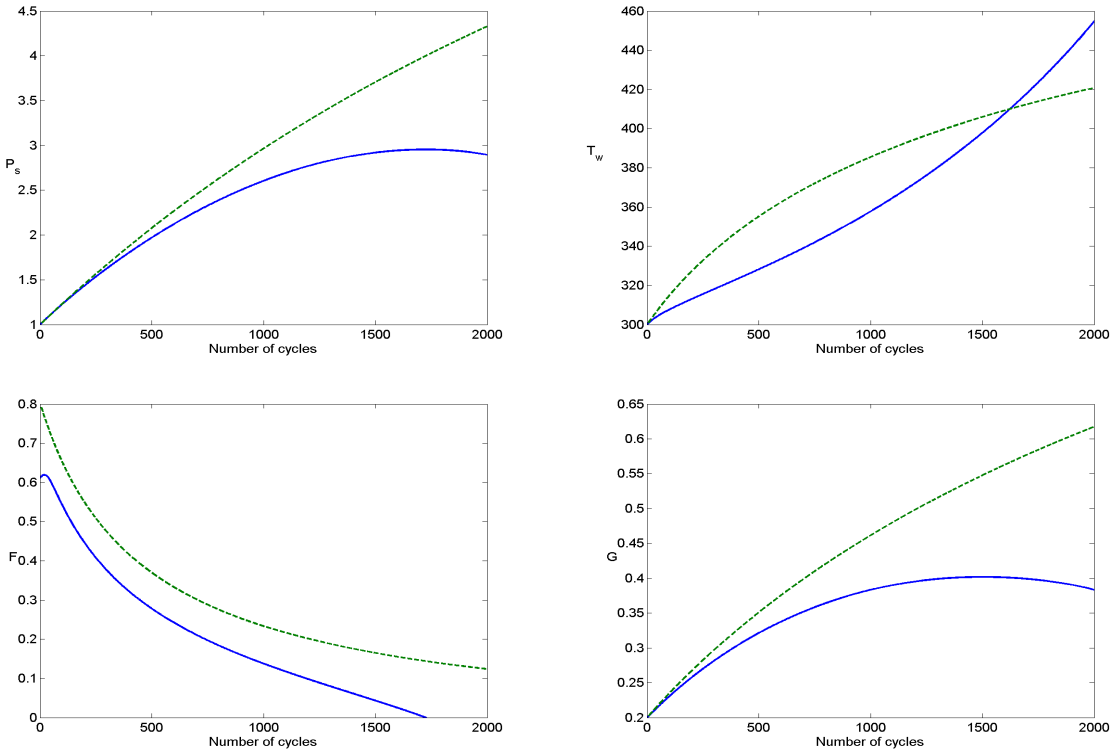

Figure 6: Storage-tank pressure, wall temperature, and piston positions F and G for a quasi-steady heat flux Q (solid line), plotted against the adiabatic result (dotted line) with $B = 0.00008$. Notice that the temperature begins to increase drastically, and that the compressor ceases operation since the exhaust valve does not open.

quasi-steady case above to find an effective relation between the storage-tank pressure P_s, wall temperature T_w, the piston locations F, G and the density ρ as

$$T_w^{(n+1)} - T_w^{(n)} = -\frac{2\,\lambda_w}{2d+d^2}\left\{B\left[T_w^{(n)}-1\right]+KQ^{(n)}\right\} \tag{58}$$

$$P_s^{(n+1)} = P_s^{(n)} + V\left\{\rho_1 F^{(n)} - (l-1)\left[\left(\gamma P_s^{(n)}-\rho_1\right)\left(1-e^{-\frac{2\,\lambda_o\alpha}{\gamma P_s^{(n)}}\,T_w^{(n)}F^{(n)}}\right)\right]\right\} \tag{59}$$

$$\begin{aligned} P_s^{(n)} = {} & \frac{p_o}{(1-l+F^{(n)})^\gamma}\,e^{\frac{\lambda_o\alpha}{\rho_o}\left\{\left[1-l+F^{(n)}\right]^2-1\right\}} + \\ & \frac{2\lambda_o\alpha T_w^{(n)}}{\left[1-l+T_w^{(n)}\right]^\gamma}\int_0^{l-F^{(n)}}(1-\bar{t})^\gamma\,e^{\frac{\lambda_o\alpha}{\rho_o}\left\{\left[1-l+F^{(n)}\right]^2-(1-\bar{t})^2\right\}}\,d\bar{t} \end{aligned} \tag{60}$$

$$\rho_1 = \frac{\rho_o}{1-l+F^{(n)}} \quad , \quad T_1 = \frac{P_s^{(n)}}{\rho_1} \tag{61}$$

$$\rho_2 = \gamma P_s^{(n)} + (\rho_1 - \gamma P_s^{(n)})e^{\frac{-2\lambda_o\alpha}{\gamma P_s^{(n)}}F^{(n)}} \quad , \quad T_2 = \frac{P_s^{(n)}}{\rho_2}\ , \tag{62}$$

$$\begin{aligned} p_o = {} & \left(\frac{1-l}{1-l+G^{(n)}}\right)^\gamma P_s^{(n)} e^{\frac{2\lambda_o\alpha}{\rho_2(1-l)}\left\{\frac{1}{2}\left[G^{(n)}-(1-l)\right]\left[G^{(n)}+(1-l)\right]\right\}} + \\ & 2\lambda_o T_w^{(n)}\left(\frac{\rho_2(1-l)}{G^{(n)}}\right)^\gamma\int_0^{G^{(n)}-(1-l)}\left(\frac{\rho_2(1-l)}{G^{(n)}-u}e^{\frac{2\lambda_o\alpha}{\rho_2(1-l)}\left\{-(1-l)u+\frac{1}{2}u^2\right\}}\right)du \end{aligned} \tag{63}$$

$$\rho_3 = \frac{\rho_2(1-l)}{G^{(n)}} \quad , \quad T_3 = \frac{p_o}{\rho_3} \tag{64}$$

$$\rho_4 = \gamma p_o + (\rho_3 - \gamma p_o)e^{-\frac{2\lambda\alpha T_w^{(n)}}{\gamma p_o}G^{(n)}} \quad , \quad T_4 = \frac{p_o}{\rho_4} \tag{65}$$

$$\begin{aligned} Q^{(n)} = {} & -\alpha\left\{T_w^{(n)} - \right. \\ & \left.\frac{1}{2}\left[(T_o+T_1)(l-F^{(n)}) + (T_1+T_2)F^{(n)} + (T_2+T_3)[G^{(n)}-(1-l)] + (T_3+T_4)(1-G^{(n)})\right]\right\} \end{aligned} \tag{66}$$

Notice that we used a crude average of the vapor temperature in the definition of the heat-transfer variable Q.

In Figure 7 we show the storage-tank pressure, the wall temperature, and the values of F and G for the adiabatic case and the cases for $\alpha = 0.125, 0.25, 0.5$. Interestingly, the behavior of these cases appears independent of the heat transfer coefficient α. In Figure 8, we see the effect of a small Biot number ($B = 0.00008$). Notice that the compressor will fail by not allowing new vapor to enter the chamber.

However, Figure 9 shows the vapor temperature of both large and small Biot numbers with $\alpha = 0.125$. Notice that the small Biot-number case results in the vapor temperature exceeding the auto-ignition point quite dramatically, while with sufficient heat transfer, the vapor temperature remains below the adiabatic rise temperature.

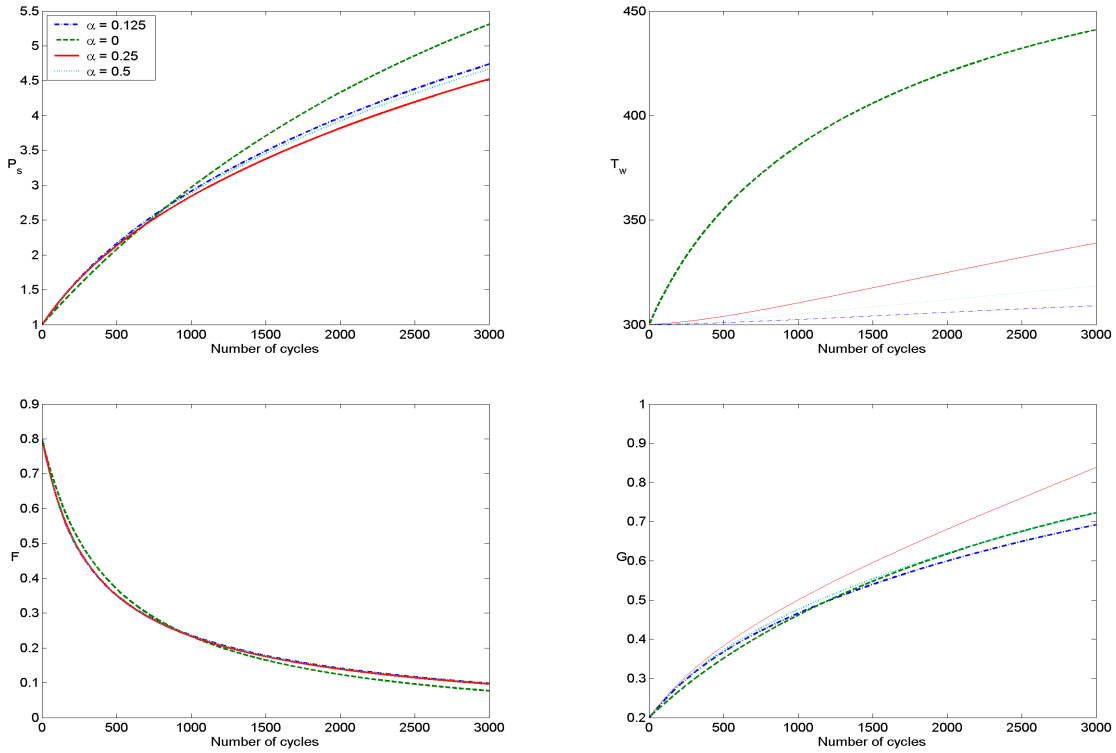

Figure 7: Storage-tank pressure, wall temperature, and piston positions F and G assuming that heat flux is proportional to the gas-wall temperature difference for $\alpha = 0.125$ (solid line), $\alpha = 0.25$ (dotted line), $\alpha = 0.5$ (dashed-dotted line), and the adiabatic case (dashed line) with $\gamma = 1.3$ and $B = 0.0008$. Notice that the behavior of this model resembles the adiabatic results resonably well.

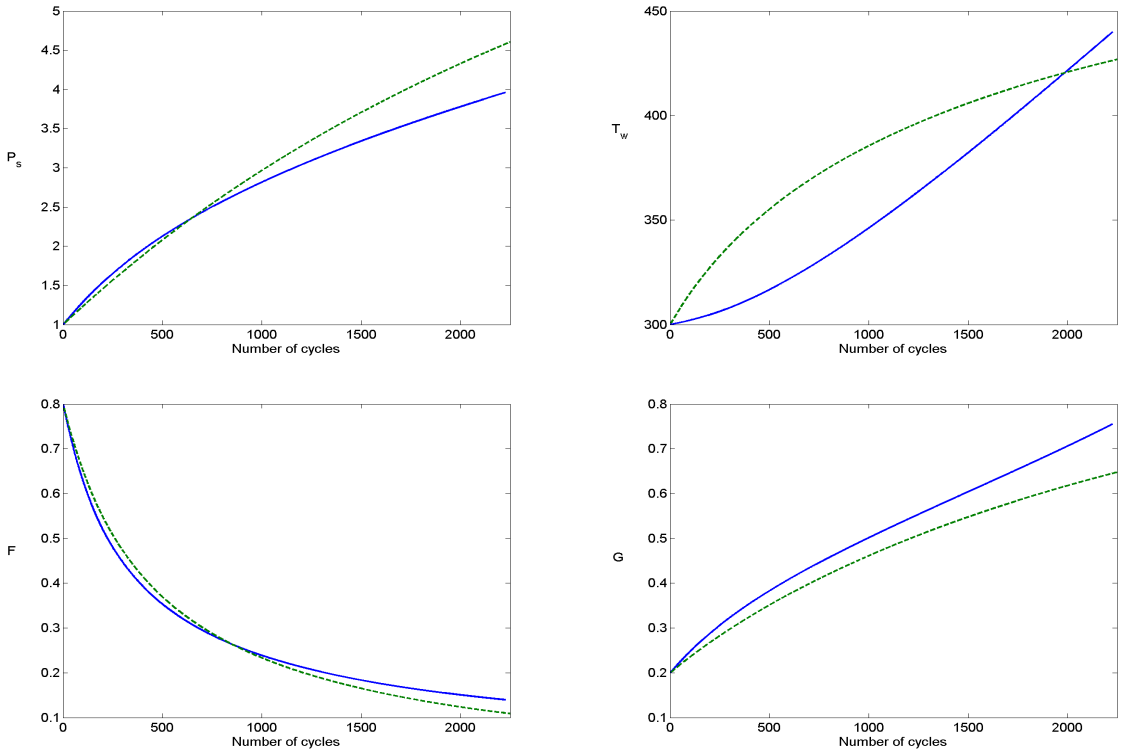

Figure 8: Storage-tank pressure, wall temperature, and piston positions F and G assuming that heat flux is proportional to the gas-wall temperature difference for $\alpha = 0.125$ (solid line) and the adiabatic case (dashed line) with $\gamma = 1.3$ and $B = 0.00008$. The wall temperature is again starting to increase markedly, while the pump will fail due to the inlet valve ceasing to open $G = 1$.

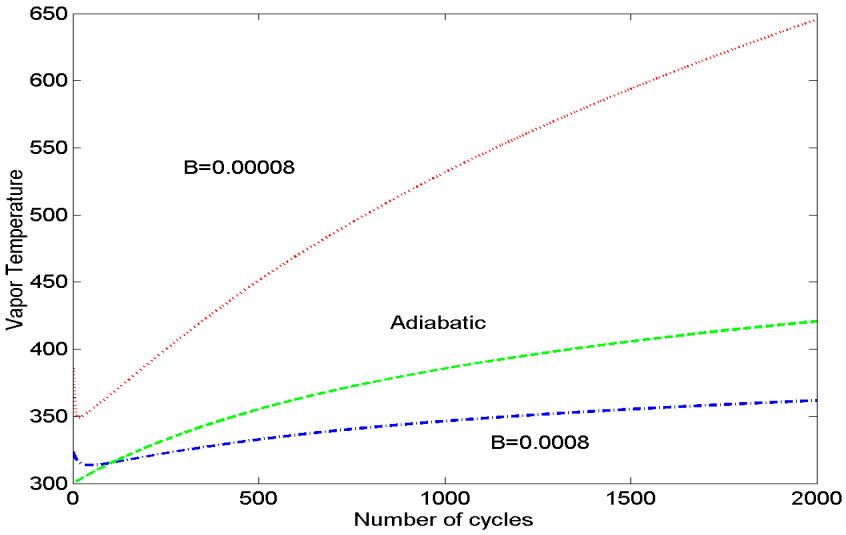

Figure 9: Vapor temperature as a function of cycles for $\alpha = 0.125$ and small Biot number ($B = 0.00008$), large Biot number ($B = 0.0008$) and the adiabatic case. Notice that initially the vapor temperature must exceed the adiabatic temperature in order to reach the storage-tank pressure. After this short transient, the long-time heat transport of the compressor wall dictates the functionality of the apparatus.

3.3 Thermal Boundary Layer near Valve Wall

At this stage, we have considered simple ordinary differential equation models that do not take into account any gradients in space of either density, temperature, or pressure of the vapor. However, during the operation of the compressor, we expect that the temperature of the valve wall, which is exposed most often to the hot vapor, will become significant. Hot spots within the vapor can result during the compression stage, since the gas within the chamber is heated, and there will be some heat transfer from the valve wall to the gas. The combination of these effects result in a localized region where the gas becomes heated above the wall and adiabatic temperature. A proper compressor design will need to take this effect into account.

To understand this phenomenon, consider the effective equations within the chamber, assuming that the walls in the radial direction are perfectly insulating.

$$\rho(T_t + uT_x) + (\gamma - 1)pu_x = \lambda_o \epsilon^2 \frac{\partial}{\partial x}\left\{\kappa(\rho)\frac{\partial T}{\partial x}\right\} \tag{67}$$

$$\frac{\partial \rho}{\partial t} + \frac{\partial}{\partial x}\{\rho u\} = 0 \tag{68}$$

$$p = \rho T \ , \tag{69}$$

with boundary conditions

$$T(x,0) = 1 \ , \ \rho(x,0) = 1 \ , u(0,t) = 0 \ , T(0,t) = T_s \ ,$$

where each quantity has been scaled based on the adiabatic conditions prior to the operation of the compressor, and $\epsilon = a/L$ is the aspect ratio of the compressor, which is small. To perform the boundary-layer analysis, we assume that

$$\xi = \frac{1-x}{\epsilon\sqrt{\lambda_o}} \ , \ u = -\epsilon\sqrt{\lambda_o}\,\bar{u} \ ,$$

which then gives us that:

$$\rho(T_t + \bar{u}T_\xi) + (\gamma - 1)p\bar{u}_\xi = \frac{\partial}{\partial \xi}\left\{\kappa(\rho)\frac{\partial T}{\partial \xi}\right\} \tag{70}$$

$$\frac{\partial \rho}{\partial t} + \frac{\partial}{\partial \xi}\left\{\rho \bar{u}\right\} = 0 \tag{71}$$

$$p = \rho T = \left(\frac{1}{1-t}\right)^\gamma \ . \tag{72}$$

Note that p, ρ, T have not been rescaled, but u has. We require at the boundary condition $\xi = 0$ that $\bar{u} = 0$, and that $T = T_s$, which is some large temperature near the maximum adiabatic rise temperature. From the numbers we expect that $1.5 < T_s < 2$ (again, scaled on 300 K). As $\xi \to \infty$, we need that

$$T \to T_{adiabatic} = \left(\frac{1}{1-t}\right)^{\gamma-1} \ , \ \bar{u} \to -\frac{\xi}{1-t} \ .$$

$$T(0,t) = T_s \ , \ T \to T_{adiabatic} \text{ as } \xi \to \infty \ .$$

From this ansatz, we can use the fact that p is given to reduce the equations. If we multiply the conservation of mass equation (71) by T and add the result to the heat equation (70), the we find that

$$p'(t) + \gamma p(t)\bar{u}_\xi = \left(k(T)T_\xi\right)_\xi \ .$$

We can integrate this equation once in ξ to find that

$$\bar{u} = \frac{1}{\gamma p(t)}\left\{-\xi p'(t) + k(T)T_\xi - q(t)\right\} \ ,$$

where $q(t)$ is an integration constant that needs to be determined from matching to the outer problem. However, we do not necessarily have enough information to perform this matching. However, if we apply the boundary condition at $\xi = 0$, we find that

$$q(t) = -k[T(0,t)]\, T_\xi(0,t) \ ,$$

or that $q(t)$ is a measure of the heat flux leaving the wall. Note that if we assume adiabatic conditions, then $q(t) = 0$.

To find the effective equation for the temperature (or density), we can use these expressions for $\bar{u}, \bar{u}_\xi$ in the conservation in mass equation (71). From this, we find that (using the equation of state (72)),

$$\frac{p'(t)T - p(t)T_t}{T^2} + \frac{p}{T}\,\bar{u}_\xi + \bar{u}\left(-\frac{p(t)}{T^2}\,T_\xi\right) = 0 \ ,$$

and after multiplying by T^2, and using the appropriate expressions for $\bar{u}, \bar{u}_\xi$, we find that

$$\gamma p(t)T_t = (\gamma - 1)p'(t)T(x,t) + \left[T\left\{k(T)T_\xi\right\}_\xi + \xi p'(t)T_\xi - k(T)\,T_\xi^2 + q(t)\,T_\xi\right] \ , \ \rho = \frac{p(t)}{T(\xi,t)} \ ,$$

subject to the boundary conditions

$$T(0,t) = T_s \ , \ T \to T_{adiabatic} \ , \ \text{as } \xi \to \infty.$$

Note that the form of the thermal conductivity of the vapor $k(T) \approx 1 + 2T$ assuming that the dominant thermal behavior is due to the nitrogen in the vapor.

In Figure 10 we show the evolution of one particular case, with $T_s = 1.5$ (we plot the results in the physical temperature, measured in Kelvin) and equally spaced intervals in time from $t = 0$ to $t = 0.5$. Notice that the development of the hot spot near the hot wall as the bulk temperature approaches its maximum adiabatic value. In Figure 11, we note that the maximum temperature value, compared to the wall temperature, increases as the wall temperature increases, from about 7% for $T_s = 1.5$ to nearly 12% for $T_s = 2$.

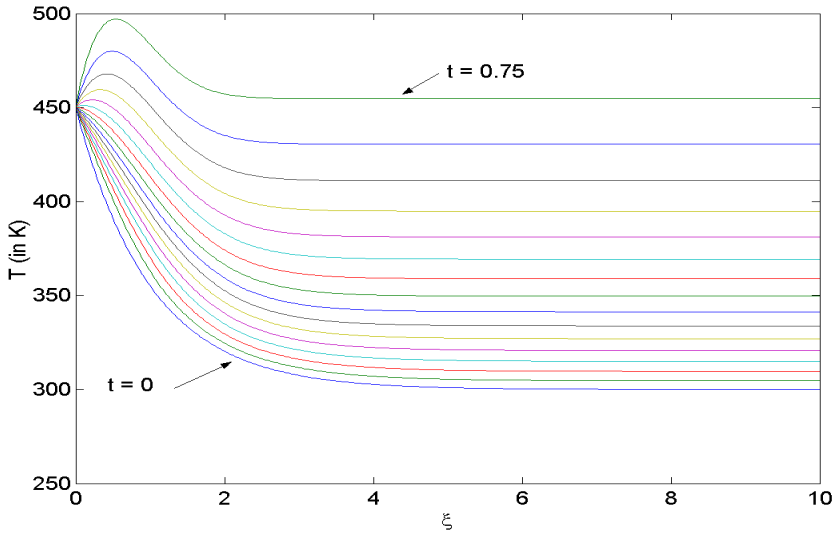

Figure 10: Temperature profiles T as a function of the inner variable ξ during the compression stage. Notice that near the end of the compression cycle that a region near the wall is heated above the adiabatic temperature.

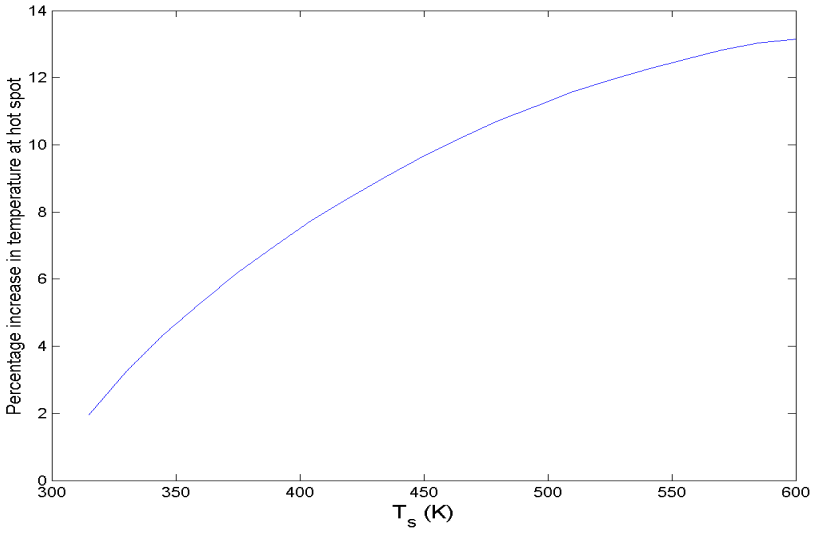

Figure 11: Percentage temperature rise within the thermal boundary layer as a function of wall temperature T_s. Notice that as the wall is heated that the relative temperature rise saturates near 12%.

4 Discussion

In this report, we have outlined systematically a one-dimensional approach addressing the feasibility of the compressor needed for the Veeder-Root emission application. From this analysis, we have found that there is a good possibility, provided that a sufficient amount of heat transport from the apparatus to the environment is attained, for a 6:1 compression ratio. This result depends however, on the assumptions that have been made in this analysis. These assumptions include that no radial effects within the compression chamber are included, no fluid-dynamical effects near the entrance or exit valves, no heat transport through the piston, no material changes that occur between the piston and the chamber wall (i.e. chafing) and no axial dependence on heat transport. However, the model presented in this work is amenable to including these effects if further analysis is warranted. Hence, the results from this report should be used as an initial guide for design: it is possible that vapor temperatures may indeed be larger than reported here when additional physical effects are included.

Further, we have found that there is a good likelihood of a hot-spot, whose temperature is approximately 10% higher than the hottest part of the apparatus. This result limits the potential of what the compressor could realistically handle.

In conclusion, the requirements for a compressor shown in Figure 1 should be attainable either through a single stage compressor (with a larger storage tank than first suggested), or by using a second compression stage. The analysis included in this work is pertinent to a multi-stage compressor solution to the problem.